Optimal Control of Internal Road Boundary for Lane-free Automated Vehicle Traffic

Milad Malekzadeh
Dynamic Systems and Simulation Laboratory
Technical University of Crete
Chania, Greece
mmalek@dssl.tuc.gr

Ioannis Papamichail
Dynamic Systems and Simulation Laboratory
Technical University of Crete
Chania, Greece
ipapa@dssl.tuc.gr

Markos Papageorgiou
Dynamic Systems and Simulation Laboratory
Technical University of Crete
Chania, Greece
markos@dssl.tuc.gr

Klaus Bogenberger
Chair of Traffic Engineering and Control
Technical University of Munich
Munich, Germany
klaus.bogenberger@tum.de

***Abstract*—This paper presents a novel traffic control action referring to virtual moving of the internal boundary of bi-directional highways for lane-free traffic of automated vehicles. Since capacity of lane-free traffic is roughly proportional to the road width, the total cross-road capacity may be shared flexibly (in space and time) between the two opposite directions according to the current bi-directional demand. In order to determine the control input, which is the road width or capacity sharing factor, an appropriate QP (Quadratic Programming) problem formulation employing the macroscopic CTM (Cell Transmission Model) is developed. Simulation results with and without control are analyzed and compared to demonstrate the potential of the proposed scheme in exploiting the available road infrastructure at unprecedented levels.**

Keywords—lane-free traffic, internal boundary control, quadratic programming, capacity sharing

I. Introduction

Vehicular traffic is crucial for the transport of persons and goods, but daily traffic congestion, entailing substantial delays, excessive environmental pollution and reduced traffic safety, has been an increasingly serious problem around the world that calls for drastic solutions. Conventional traffic management measures are valuable [1], [2] but not always sufficient to tackle the heavily congested traffic conditions, which must be addressed in a more comprehensive way that exploits gradually emerging and future ground-breaking capabilities of vehicles and the infrastructure. During the last decade, there has been an enormous effort by the industry and by numerous research institutions to develop and deploy a variety of vehicle automation and communication systems that are revolutionizing the vehicle capabilities [3].

A recent paper [4] launched the TrafficFluid concept, which is a novel paradigm for vehicular traffic, applicable at high levels of vehicle automation and communication and high penetration rates, as expected to prevail in the not-too-far future. The TrafficFluid concept is based on the following two combined principles: (1) Lane-free traffic, whereby vehicles are not bound to fixed traffic lanes, as in conventional traffic, but may drive anywhere on the 2-D surface of the road; (2) Vehicle nudging, whereby vehicles communicate their presence to other vehicles in front of them, and this may exert a "nudging" effect on the vehicles in front, i.e. vehicles in front may experience (apply) a pushing influence. Several advantages and challenges related to this novel traffic paradigm are discussed in [4] and [5]. This paper exploits the lane-free property of TrafficFluid, i.e. the possibility for vehicles to drive on the 2-D road surface without being bound to lanes. As demonstrated in a small experiment in [4], and is also intuitively sensible, lane-free traffic implies that the flow capacity may exhibit incremental (increasing or decreasing) changes in response to corresponding incremental (widening or narrowing) changes of the road width.

Consider a road or highway with two opposite traffic directions, where connected and automated vehicles (CAV) are driving. The total carriageway capacity (for both directions) could be shared among the two directions in a flexible way according to the prevailing bi-directional demand, so as to maximize the infrastructure exploitation congestion in either direction. Flexible capacity sharing may be achieved via virtual moving of the internal boundary, which separates the two traffic directions, and corresponding communication to the CAV to respect the changed internal boundary. This way, the carriageway's width portion (and total capacity share) assigned to each traffic direction can be changed in space and time (subject to constraints) according to an appropriate control strategy, as illustrated in Fig. 1.

The idea of sharing the total road capacity among the two traffic directions is not new and has been occasionally employed for conventional lane-based traffic, typically offline or manually [6]. The measure is known as tidal flow or reversible lane control, and its main principle is to adapt the total available cross-road supply to the bi-directional demand. Its most basic form is the steady allocation of one (or more) lanes of one direction to the opposite direction for a period of time (ranging from few hours to many days) in the aim of addressing abnormal traffic supply or demand. More advanced reversible lane systems may operate in real time to balance delays on both sides of a known bottleneck (e.g. bridge, tunnel) by assigning a lane to the each of the two directions in alternation in response to the prevailing traffic conditions. To this end, optimal control or feedback control algorithms of various types are proposed (see e.g. [7], [8]).

Reversible lanes have also been considered in connection with lane-based CAV driving. Reference [9] uses the system optimal dynamic traffic assignment models for a single destination [10] and for more general networks [11], that utilize the Cell Transmission Model (CTM) [12]. Lanes are introduced as integer variables, and the problem is formulated as a mixed integer linear programming (MILP)

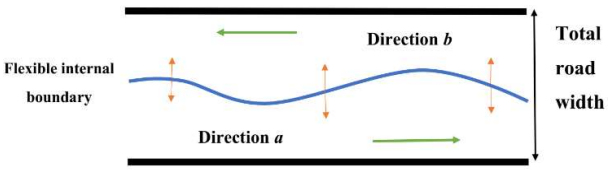

Fig. 1. Space-time flexible internal road boundary

The research leading to these results has received funding from the European Research Council under the European Union's Horizon 2020 Research and Innovation programme/ ERC Grant Agreement n. [833915], project TrafficFluid.

978-1-7281-8995-6/21/$31.00 ©2021 IEEE

problem that has, however, high (exponential) complexity due to the many integers variables involved. This model was also used in [13] for a single link utilizing stochastic demand as a Markov decision process. The MILP problem is solved using a heuristic and is incorporated within a UE routing problem.

Lane-based tidal flow control systems may be very useful for certain situations (e.g. work zones), but they face a number of difficulties that limit their widespread use. Most importantly, the resolution of infrastructure sharing among the two traffic directions cannot be higher than one lane, which is not sufficiently fine-grained for most traffic situations. A second drawback is about reversible lane implementation; whenever a reversible lane switch to the opposite direction is decided, a time-delay (corresponding to the travel time on the reversible lane) must be respected, before actually opening the lane to the opposite direction, so as to allow for the evacuation of the lane and avoid simultaneous opposite-direction movements. In addition, a reversible lane must extend over sufficient length (minimum of few kilometers) to avoid counter-problems due to merging or diverging traffic.

Even in the future CAV traffic, however, some of the mentioned difficulties would persist in lane-based conditions, notably the low capacity sharing resolution, the merging nuisance and, last not least, the complex (integer-based) nature of the corresponding optimization problems that hinder real-time feasibility. In contrast, in a lane-free CAV traffic environment, the mentioned difficulties are largely mitigated. Specifically:

- The resolution of infrastructure sharing among the two directions can be high.
- The smooth driving of CAV in a lane-free road surface allows for the internal boundary to be a smooth space-function, as illustrated in Fig. 1.
- Due to moderate changes of the internal boundary over time and space and the lack of physical boundary, the aforementioned safety-induced time-delay, required to avoid opposite movements on the same road surface, may be small.
- As practiced in this paper, the resulting optimization problems include only real-valued variables (no integers are necessary) and may therefore be solved very efficiently, so as to be readily real-time feasible.

Thanks to these characteristics, real-time internal boundary control for lane-free CAV traffic may be broadly applicable to the high number of arterial or highway infrastructures that feature unbalanced demands during the day in the two traffic directions, so as to strongly mitigate or even avoid congestion.

This paper proposes a macroscopic model-based optimization scheme to elaborate on and demonstrate the characteristics of internal boundary control. The well-known CTM [12] is employed to this end, leading to a convex Quadratic Programming (QP) problem. A carefully designed simulation scenario highlights some interesting implications of this innovative control measure.

The rest of the paper is organized as follows: Section II outlines some preliminary issues related to the problem at hand; including the CTM-based optimal control problem is given in Section III. Transforming the formulation to QP problem form is presented in Section IV. Simulation results are delivered in Section V and, following this, some conclusions and discussion are included in Section VI.

II. PRELIMINRIES

Various dynamic traffic flow models have been employed in the formulation of optimal control problems, among which a simple but realistic possibility is CTM [12], see [10], [14] for CTM-based optimal control formulations (among many others). CTM is a first-order model with triangular FD, which attains a space-time discretized form via application of the Godunov numerical scheme [15]. The main advantage of CTM, when used within an optimal control setting, is that it may lead to a convex, hence globally optimizable, linear or quadratic optimization problem, which can be solved numerically using very efficient available codes. The reason behind this property is that the nonlinearities that every traffic flow model must necessarily feature to realistically reflect the traffic flow dynamics, have, in CTM, a piecewise linear form that is amenable to linear constraints for the optimization problem and, hence, to a convex admissible region.

Lane-free traffic is not expected to give rise to structural changes of existing macroscopic models. It is reasonable to assume, as also supported by results in [4], [16], [17], that notions and concepts like the conservation equation, the fundamental diagram, as well as moving traffic waves will continue to characterize macroscopic traffic flow modelling in the case of CAV lane-free traffic. By the same token, specific physical traffic parameters, such as free speed, critical density, flow capacity, jam density, are also relevant for lane-free traffic, but may of course take different values than in lane-based traffic. In the next section, we will use CTM, appropriately adjusted to incorporate the internal boundary control, so as to cast the control problem in the form of a convex Quadratic Programming (QP) problem.

In the present context, it is crucial to elaborate on the impact of internal boundary control on the respective Fundamental Diagrams (FDs) of the two opposite traffic directions, which we call directions a and b, respectively (Fig. 1). Let us assume that directions a and b are assigned respective road widths (in m) $w^a = \varepsilon \cdot w$ and $w^b = (1-\varepsilon)\cdot w$, where $0 \le \varepsilon \le 1$ is the sharing factor and w is the total road width (for both directions). Let $Q(\rho)$, where ρ is the traffic density in veh/km, be the total FD (both directions) of a highway section, which would prevail if the whole carriageway would be assigned to only one of the two opposite traffic directions (i.e. for ε equal 0 or 1), with total critical density ρ_{cr}, total capacity q_{cap} and total jam density $\rho_{\max}$. Let us consider the case of partial road sharing, i.e. $\varepsilon_{\min} \le \varepsilon \le \varepsilon_{\max}$, where $\varepsilon_{\min}, \varepsilon_{\max} \in (0,1)$ are appropriate bounds to be specified later. We want to derive the corresponding FDs and parameter values for the two directions a and b. It is not difficult to deduce (see also [18] for a more general derivation) that the FDs for the two directions, which are functions of ε, are given by

$$\begin{aligned} Q^a(\rho^a, \varepsilon) &= \varepsilon \cdot Q(\rho^a / \varepsilon), \\ Q^b(\rho^b, \varepsilon) &= (1-\varepsilon)\cdot Q(\rho^b / (1-\varepsilon)) \end{aligned} \tag{1}$$

where ρ^a and ρ^b (in veh/km) are the respective densities of the two directions.

Let us subdivide a highway stretch holding two opposite traffic directions a and b in n road sections, each some 500 m in length. The total road width, which is assumed constant over all sections for simplicity, can be flexibly shared among the two directions in real time. As the sharing may be different for every section, we have corresponding sharing factors ε_i, $i=1,2,.....,n$; and (1) applies to each section. As a consequence, the total section capacity, as well as the critical density and jam density, are shared among traffic directions a and b according to

$$\begin{aligned} q^a_{i,cap}(\varepsilon_i)=\varepsilon_i\cdot q_{cap},\ q^b_{i,cap}(\varepsilon_i)=(1-\varepsilon_i)\cdot q_{cap},\\ \rho^a_{i,cr}(\varepsilon_i)=\varepsilon_i\cdot \rho_{cr},\ \rho^b_{i,cr}(\varepsilon_i)=(1-\varepsilon_i)\cdot \rho_{cr},\\ \rho^a_{i,\max}(\varepsilon_i)=\varepsilon_i\cdot \rho_{\max},\ \rho^b_{i,\max}(\varepsilon_i)=(1-\varepsilon_i)\cdot \rho_{\max}. \end{aligned} \tag{2}$$

The corresponding changes of the triangular FD that may occur at each section and traffic direction are illustrated in Fig. 2. More specifically, when the value of control input is 0.5, i.e., the flow capacities of the two directions are equal, their FDs are "nominal" (blue line with $(.)^N$ parameters); when the control input is different than 0.5, we get two FDs: the extended one (green line with $(.)^E$ parameters) applies to the direction that is assigned higher width; and the reduced, complementary FD (orange line with $(.)^R$ parameters) applies to the other direction that is assigned less flow capacity. Based on (2), all FD parameters of a section change, whenever it is decided to change the corresponding sharing factor in real time.

The control time step T_c does not need to be equal to the model time step T, but is assumed to be a multiple of T, in which case, the control time index is given by $k_c=\lfloor kT/T_c \rfloor$. It is noted that the notation $\varepsilon(k_c)$ indicates that the specific sharing factor is applied for the duration of the control time interval $[k_c\cdot T_c,(k_c+1)\cdot T_c)$.

For the internal boundary control problem, we would like to disallow the utter closure of either direction; hence, the assigned road width in either direction should never be smaller than the widest vehicles driving on the road, hence we have the constraints

$$0<\varepsilon_{i,\min}\le\varepsilon_i\le\varepsilon_{i,\max}<1 \tag{3}$$

where $\varepsilon_{i,\min}\cdot w$ and $(1-\varepsilon_{i,\max})\cdot w$ are the minimum admissible widths to be assigned to directions a and b, respectively.

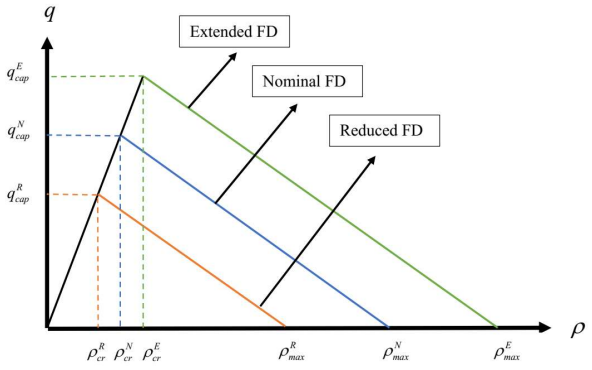

Fig. 2. The triangular fundamental diagram with flexible internal boundary

Another restriction to be applied to the sharing factors concerns the time-delay needed to evacuate traffic on the direction that receives a restricted width, compared with the previous control time step. This time-delay is small in lane-free CAV traffic with moderate changes of the sharing factors that are applied to short sections. This time-delay is omitted here for simplicity, but it is considered in a more comprehensive work [18].

III. CTM-BASED OPTIMAL CONTROL PROBLEM

We are now ready to present the CTM equations, considering the changing sharing factors. We recall that we consider a highway stretch with n sections, with respective lengths L_i. Traffic flows from section 1 to section n for direction a; and from section n to section 1 for direction b (see Fig. 3 for an example). We denote ρ^a_i, $i=1,2,....,n$, the traffic density of section i, direction a; and ρ^b_i, $i=1,2,....,n$, the traffic density of section i, direction b. Similarly, we have the mainstream exit flows of section i being denoted q^a_i for direction a and q^b_i for direction b. Thus, q^a_0 is the feeding upstream mainstream inflow for direction a ; and q^b_{n+1} is the feeding upstream mainstream inflow for direction b. In addition, every section may have an on-ramp or an off-ramp at its upstream boundary. The on-ramp flow (if any) for section i, direction a, is denoted r^a_i; and the on-ramp flow (if any) for section i, direction b, is denoted r^b_i. The off-ramp flow (if any) of section i, direction a, is calculated based on known exit rates β^a_i multiplied with the upstream-section flow, i.e. $\beta^a_i q^a_{i-1}$; and the off-ramp flow (if any) of section i, direction b, is calculated based on known exit rates β^b_i multiplied with the upstream-section flow, i.e. $\beta^b_i q^b_{i+1}$.

The conservation equation for direction a is presented as follows

$$\begin{aligned} &\rho^a_i(k+1)=\rho^a_i(k)+\frac{T}{L_i}((1-\beta^a_i)q^a_{i-1}(k)-q^a_i(k)+r^a_i(k)),\\ &i=1,2,...,n. \end{aligned} \tag{4}$$

According to CTM, the traffic flows are obtained as the minimum of demand and supply functions, except for the last section, where we consider only the demand function, as we assume that the downstream traffic conditions are uncongested. So, we have

$$\begin{aligned} &q^a_i(k)=\min\left\{Q_D(\rho^a_i(k),\varepsilon_i(k_c)),\frac{Q_S(\rho^a_{i+1}(k),\varepsilon_{i+1}(k_c))}{(1-\beta^a_{i+1})}-r^a_{i+1}(k)\right\},\\ &i=1,2,....,n-1,\\ &q^a_n(k)=Q_D(\rho^a_n(k),\varepsilon_i(k_c)), \end{aligned} \tag{5}$$

where the demand and supply functions are given by

$$\begin{aligned} &Q_D(\rho^a_i(k),\varepsilon_i(k_c))=\min\left\{\varepsilon_i(k_c)q_{cap},v_f\rho^a_i(k)\right\},\\ &i=1,2,...,n,\\ &Q_S(\rho^a_i(k),\varepsilon_i(k_c))=\min\left\{\varepsilon_i(k_c)q_{cap},w_s(\varepsilon^a_i(k_c)\rho_{\max}-\rho^a_i(k))\right\},\\ &i=1,2,...,n-1, \end{aligned} \tag{6}$$

where v_f is the free speed (which is assumed equal for all sections for simplicity) and w_s is the back-wave speed.

Similarly, for direction b we have

$$\rho_i^b(k+1) = \rho_i^b(k) + \frac{T}{L_i}((1-\beta_i^b)q_{i+1}^b(k) - q_i^b(k) + r_i^b(k)), \quad i = 1,2,...,n \tag{7}$$

and the flows are given by

$$q_i^b(k) = \min\left\{Q_D(\rho_i^b(k),\varepsilon_i(k_c)), \frac{Q_S(\rho_{i-1}^b(k),\varepsilon_{i-1}(k_c))}{(1-\beta_{i-1}^b)} - r_{i-1}^b(k)\right\}, \quad i = 2,3,....,n,$$
$$q_1^b(k) = Q_D(\rho_1^b(k),\varepsilon_i(k_c)), \tag{8}$$

where

$$Q_D(\rho_i^b(k),\varepsilon_i(k_c)) = \min\left\{(1-\varepsilon_i(k_c))q_{cap}, v_f\rho_i^b(k)\right\}, \quad i = 1,2,...,n,$$
$$Q_S(\rho_i^b(k),\varepsilon_i(k_c)) = \min\left\{(1-\varepsilon_i(k_c))q_{cap}, w_s((1-\varepsilon_i(k_c))\rho_{\max} - \rho_i^b(k))\right\}, \quad i = 2,3,...,n. \tag{9}$$

IV. Quadratic Programming Formulation

The conservation equations (4) and (7) are linear, but, due to the presence of the min-operator in (5), (6), (8) and (9) (9), the CTM flow equations presented in the previous section are nonlinear. In this regard, (5) and (6) of direction a yield the following four inequalities

$$q_i^a(k) \le v_f\rho_i^a(k), \tag{10}$$

$$q_i^a(k) \le \varepsilon_i(k_c)q_{cap}^{total}, \tag{11}$$

$$q_i^a(k) \le \frac{w_s}{(1-\beta_{i+1}^a)}(\varepsilon_{i+1}(k_c)\rho_{\max}^{total} - \rho_{i+1}^a(k)), \tag{12}$$

$$q_i^a(k) \le \frac{\varepsilon_{i+1}(k_c)q_{cap}^{total}}{(1-\beta_{i+1}^a)}, \tag{13}$$

where (10) and (11) define the demand function while (12) and (13) imply the supply function. Similarly, for direction b we have

$$q_i^b(k) \le v_f\rho_i^b(k), \tag{14}$$

$$q_i^b(k) \le (1-\varepsilon_i)(k_c)q_{cap}^{total}, \tag{15}$$

$$q_i^b(k) \le \frac{w_s}{(1-\beta_{i-1}^b)}((1-\varepsilon_{i-1}(k_c))\rho_{\max}^{total} - \rho_{i-1}^b(k)), \tag{16}$$

$$q_i^b(k) \le \frac{(1-\varepsilon_{i-1})q_{cap}^{total}}{(1-\beta_{i-1}^b)}. \tag{17}$$

To complete the QP problem formulation, we need to specify a quadratic cost function. The cost function must be defined in such a way that the main control goal as well as operational aspects of implementation are considered. In this sense, we define the cost function as follows

$$J = T\sum_{k=1}^{K}\sum_{i=1}^{n}\left(L_i\rho_i^a(k) + L_i\rho_i^b(k)\right) + w_1\sum_{k_c=1}^{K_c-1}\sum_{i=1}^{n}\left(\varepsilon_i(k_c) - \varepsilon_i(k_c-1)\right)^2 + w_2\sum_{k_c=0}^{K_c-1}\sum_{i=2}^{n}\left(\varepsilon_i(k_c) - \varepsilon_{i-1}(k_c)\right)^2 + w_3\sum_{k_c=0}^{K_c-1}\sum_{i=2}^{n}\left(\varepsilon_i(k_c) - 0.5\right)^2. \tag{18}$$

The cost function extends over a time horizon of K model time steps or K_c control time steps, where $K_c = K\cdot T/T_c$ and it includes four terms. The first term presents the Total Time Spent (TTS) as a most important term for the pursued traffic flow efficiency maximization. The second and third terms aim at penalizing the variation of the control input in consecutive time-steps and segments, respectively, so as to obtain a smooth control input in space and time. The last term is considered in order to limit deviations of the sharing factors form the nominal value of 0.5, which is the equal share for both directions. This completes the QP problem formulation, which may now be used to address the internal boundary moving problem.

V. Simulation Test

The motorway stretch considered for simulation testing of the proposed concept is displayed in Fig. 3. Its length is 3 km and it is subdivided in 6 sections of equal length.

The modelling time step is $T = 10\,\text{s}$, and the control time step $T_c = 60\,\text{s}$. The considered time horizon is 1 h, hence $K = 360$ and $K_c = 60$. The utilized CTM parameters are $v_f = 100\,\text{km/h}$ and $w_s = 12\,\text{km/h}$; while the total cross-road capacity to be shared among the two directions is $q_{\max} = 12{,}000\,\text{veh/h}$. The upper and lower bounds for the sharing factors, so as to avoid utter blocking of any of the two directions, are equal for all sections and are given the values $\varepsilon_{\min} = 0.16$ and $\varepsilon_{\max} = 0.84$. The exit rates of the off-ramps are both equal to 0.1.

The demand flows for the investigated scenario are displayed in Fig. 4 for both directions. It may be seen that the two directions feature respective peaks in their upstream mainstream demands that are slightly overlapping. In addition, the on-ramp demands are constant, with the on-

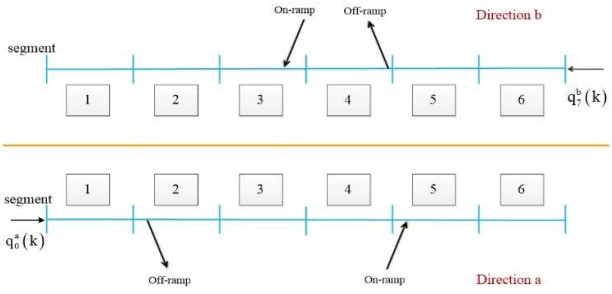

Fig. 3. The considered highway stretch

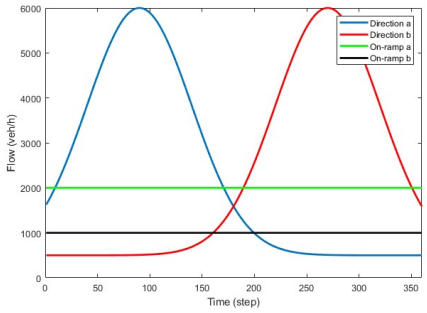

Fig. 4. Demand flows of each direction

ramp demand in direction a being higher than in direction b.

The simulation results for the no-control case will be presented first, followed by the results obtained with optimal internal boundary control resulting from the solution of the corresponding QP problem. The weight parameters used in the cost function of the QP problem for the respective terms are $w_1 = 10^{-4}, w_2 = 10^{-4}, w_3 = 10^{-5}$.

Using the entering flows of the proposed scenario in the CTM equations with constant internal boundary at $\varepsilon_i = 0.5$ for all sections, we obtain the simulation results of the no-control case with a TTS value equal to 209.8 veh·h. Fig. 5 displays the corresponding spatio-temporal density evolution. More precisely, the variable displayed for each direction is the relative density, defined as $\tilde{\rho}^a(k) = \rho^a(k) / \rho^a_{cr}(k) = \rho^a(k) / (\varepsilon\ (k-1)\rho_{cr})$ for direction a and $\tilde{\rho}^b(k) = \rho^b(k) / \rho^b_{cr}(k) = \rho^b(k) / ((1-\varepsilon\ (k-1))\rho_{cr})$ for direction b. Note that density (in veh/h) by itself is not sufficient, in the internal boundary control environment, to distinguish between under-critical and congested traffic conditions, because the critical density is also changing according to the applied control. Of course, the critical density is not changing in the no-control case, but we use already here relative densities for consistency with the control case. According to the definition, relative density values lower than 1 refer to uncongested traffic; while values higher than 1 refer to congested traffic; clearly, when the relative density equals 1, and the downstream section is uncongested, we have capacity flow at the corresponding section.

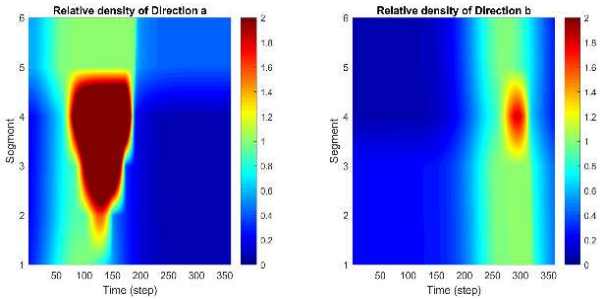

Fig. 5. Relative density of the two directions in the no-control case

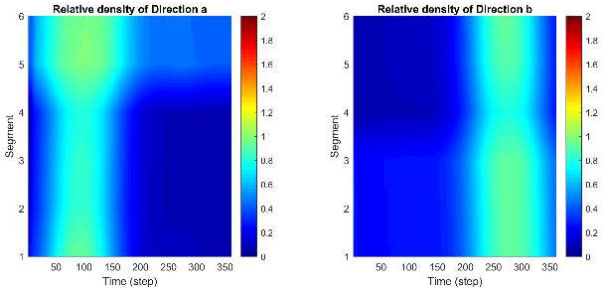

Fig. 6. Relative density of the two directions in the control case

Fig. 5 shows that, heavy congestion is created in section 5 for direction a due to the strong ramp inflow, in combination with the increased mainstream demand, at around $k = 60$. The congestion tail propagates backwards, reaching up to section 2, and the congestion is dissolved at around $k = 200$, thanks to the rapid decrease of the mainstream demand (Fig. 4). In direction b, we have also a congestion being triggered by the increasing mainstream demand, in combination with the on-ramp flow, in section 3 at around $k = 250$. Due to lower on-ramp flow, this congestion is smaller than in direction a; it spills back up to section 5 and dissolves at around $k = 330$.

Next, the simulation results in the presence of the controller will be presented. The spatio-temporal evolution of the relative densities in Fig. 6 confirm that the proposed capacity sharing strategy is effective in alleviating, in this case utterly avoiding, the congestion.

Figs. 7, 8, 9 display more detailed information for this case. Specifically, each figure holds the results of two respective sections; for each section, we provide three

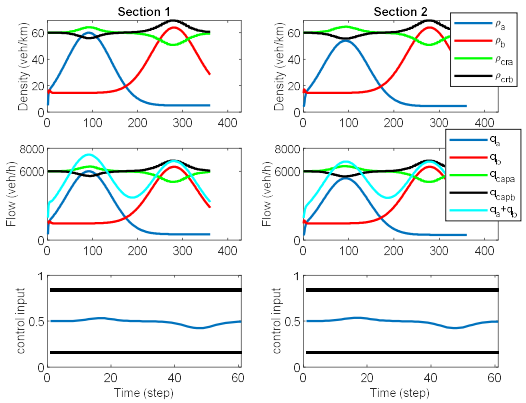

Fig. 7. Density, flow and control trajectories in the control case (sections 1 and 2)

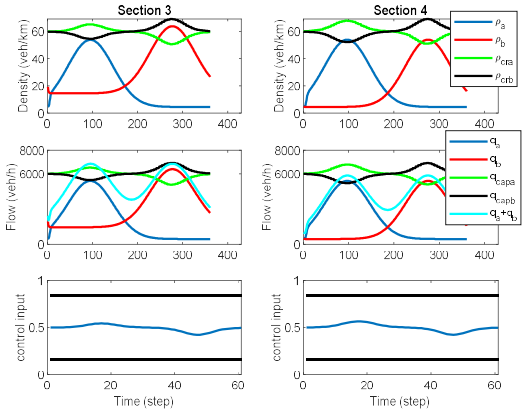

Fig. 8. Density, flow and control trajectories in the control case (sections 3 and 4)

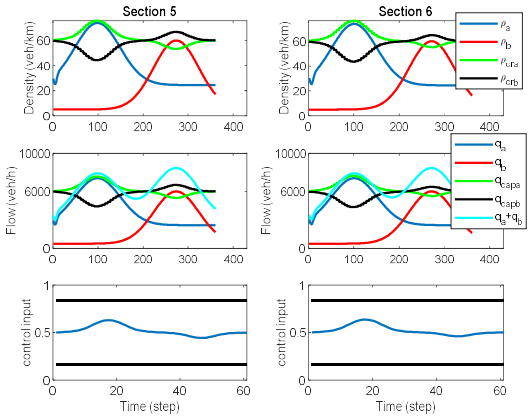

Fig. 9. Density, flow and control trajectories in the control case (sections 5 and 6)

diagrams:

- The first diagram shows the two traffic densities (in veh/km), for directions a and b, along with the corresponding two critical densities, which are changing according to the sharing factor in the section.
- The second diagram shows the two traffic flows, for directions a and b, and the corresponding two capacities, which are changing according to the sharing factor in the section. In addition, the sum of both flows is also displayed (cyan curve).
- The third diagram shows the two sharing factors. Note that the time axis in this case displays the control time steps k_c.

The displayed results confirm that densities (flows) are always lower than the respective critical densities (capacities) in all sections and in both directions; hence traffic conditions are always and everywhere under-critical. In fact, the total-flow curve (for both directions) does not reach the total carriageway capacity (of 12,000 veh/h) at any time anywhere. In short, congestion is utterly avoided. The sharing factor trajectories of the sections reveal that this excellent outcome is enabled via a smooth swapping over time of the capacity assigned to the two directions, whereby more capacity is assigned to direction during the first half of the time horizon and vice-versa for the second half, so as to accommodate the changing respective demands and their peaks. The resulting TTS value is equal to 164.9 veh·h that is an improvement of 21.4 % over the no-control case. Since no congestion is formed in the no-control case, the reduction in travel delay is 100 %.

VI. Conclusion

In this study, internal boundary moving for *lane-free* traffic has been addressed and investigated. To this end, quadratic programming has been employed as a fast and effective tool to design the dynamic and space-dependent sharing factor between two traffic directions. The simulation results have been presented with and without control, and their comparison, both qualitative and quantitative (based on TTS values), confirm the effectiveness of the proposed measure and scheme.

References

[1] M. Papageorgiou, C. Diakaki, V. Dinopoulou, A. Kotsialos, and Y. Wang, "Review of road traffic control strategies," Proc. of the IEEE, vol. 91(12), pp. 2043–2067, 2003.

[2] A.A. Kurzhanskiy, and P. Varaiya, "Active traffic management on road networks: a macroscopic approach," Philosophical Transactions of the Royal Society A: Mathematical, Physical and Engineering Sciences, vol. 368(1928), pp. 4607–4626, 2010

[3] C. Diakaki, M. Papageorgiou, I. Papamichail, and I. Nikolos, "Overview and analysis of vehicle automation and communication systems from a motorway traffic management perspective," Transportation Research Part A: Policy and Practice, vol. 75, pp. 147–165, 2015.

[4] M. Papageorgiou, K.S. Mountakis, I. Karafyllis, I. Papamichail, and Y. Wang, "Lane-free artificial-fluid concept for vehicular traffic," Proceedings of the IEEE, 109(2), pp. 114-121, 2021.

[5] M. Papageorgiou, K.S. Mountakis, I. Karafyllis, and I. Papamichail, "Lane-free artificial-fluid concept for vehicular traffic," arXiv preprint arXiv:1905.11642, 2019.

[6] P.B. Wolshon and L. Lambert, "Convertible roadways and lanes: a synthesis of highway practice," DC: Transportation Research Board National Research Council (vol. 340), 2004.

[7] J.R.D. Frejo, I. Papamichail, M. Papageorgiou, and E.F. Camacho, 2015. "Macroscopic modeling and control of reversible lanes on freeways," IEEE Transactions on Intelligent Transportation Systems, vol. 17(4), pp. 948-959, 2015.

[8] K. Ampountolas, J.A dos Santos, and R.C. Carlson, "Motorway tidal flow lane control," IEEE Transactions on Intelligent Transportation Systems, vol. 21(4), pp. 1687–1696, 2020.

[9] M. Duell, M.W. Levin, S.D. Boyles, and S.T. Waller, "Impact of autonomous vehicles on traffic management: Case of dynamic lane reversal," Transportation Research Record, no. 2567, pp. 87–94, 2016.

[10] A.K. Ziliaskopoulos, "A linear programming model for the single destination system optimum dynamic traffic assignment problem," Transportation Science, vo. 34(1), pp. 37–49, 2000.

[11] Y. Li, S.T. Waller, and A. Ziliaskopoulos, "A decomposition scheme for system optimal dynamic traffic assignment models," Networks and Spatial Economics, vol. 3(4), pp.441–455, 2003.

[12] C.F. Daganzo, "The cell transmission model: A dynamic representation of highway traffic consistent with the hydrodynamic theory," Transportation Research Part B: Methodological, vol. 28(4), pp. 269–287, 1994.

[13] M.W. Levin and S.D. Boyles, "A cell transmission model for dynamic lane reversal with autonomous vehicles," Transportation Research Part C: Emerging Technologies, vol. 68, pp. 126–143, 2016.

[14] C. Roncoli, M. Papageorgiou, and I. Papamichail, "Traffic flow optimisation in presence of vehicle automation and communication systems–Part I: A first-order multi-lane model for motorway traffic," Transportation Research Part C: Emerging Technologies, vol. 57, pp. 241–259, 2015.

[15] J.P. Lebacque, "The Godunov scheme and what it means for first order traffic flow models," International Symposium on Transportation and Traffic Theory, pp. 647–677, 1996.

[16] B. Bhavathrathan and C. Mallikarjuna, "Evolution of macroscopic models for modeling the heterogeneous traffic: an Indian perspective," Transportation Letters, vol. 4(1), pp. 29–39, 2012.

[17] G. Asaithambi, V. Kanagaraj, and T. Toledo, 2016. "Driving behaviors: Models and challenges for non-lane based mixed traffic," Transportation in Developing Economies, vol. 2, no.19, 2016.

[18] M. Malekzadeh, I. Papamichail, M. Papageorgiou, K. Bogenberger, "Optimal internal boundary control of lane-free automated vehicle traffic," arXiv preprint arXiv:2008.10255, 2020.